High Shear Rheology of Paper Coating Colors – More Than Just Viscosity

Norbert Willenbacher, Haryutun Hanciogullari, Hans G. Wagner*

Capillary viscometry is used to characterize viscosity, entrance pressure loss and apparent wall slip of paper coating colors at high shear rates. Special emphasis is laid on the dependence of these phenomena on solids content in order to account for changes in the rheology due to the dewatering of the color during the coating process. Coating colors with substantially different runnability have been investigated. Differences in apparent wall slip and high shear viscoelasticity (manifesting itself in extremely high entrance pressure losses) are observed at increased concentration, even if these phenomena do not show up at the initial solids content. Poor runnability is observed when viscosity, entrance pressure loss and wall slip increase strongly with increasing solids content. But all rheological features change simultaneously with the coating color recipe and it is not possible to separate out the contribution of the particular rheological features on the runnability of the coating colors or to correlate the runnability to a single rheological parameter. Future work will have to focus on a numerical analysis of the blade coating process taking into account all the rheological features described here. First simulations including slip at the color/blade interface indicate that wall slip may cause severe runnability problems, at least when the apparent slip velocity exceeds the web velocity.

1 Introduction

Paper is coated with mineral-based aqueous colors in order to improve its appearance and printability. Blade coating is one of the most important application techniques for high-speed paper coating. For economic reasons machine speeds have been increased up to 2000 m/min. But these efforts are counteracted by a variety of runnability problems including bleeding, formation of solid depositions on the blade, poor coat weight control or web breaks increasing the downtime of the paper machine.

A major goal of coating color development is to minimize these runnability problems. A key parameter controlling the application behavior is the rheology of the colors. Therefore, the rheological properties and, since shear rates up to $10^7\ s^{-1}$ may be reached under the blade, especially the high shear viscosity of such colors have been studied intensively over the years [1–5].

It has turned out that high speed runnability is controlled by a complex interrelationship between coating rheology and other coating formulation properties like water retention as well as machine parameters (e.g., blade stiffness, blade angle, speed) and basestock properties (e.g., porosity, compressibility, roughness and wetting behavior) [4, 6, 7]. Therefore, it is not possible to predict runnability simply from laboratory rheological measurements.

Recently, it has been tried to determine the relevant runnability parameters by a detailed modelling of the coating process using computational fluid dynamics (CFD) [4].

Nevertheless, rheology is the essential coating color property entering directly into this numerical calculations. Therefore, a thorough rheological characterization of the colors under consideration is imperative.

Here, we present rheological data on four coating colors with substantially different runnability. Apart from the high shear viscosity, viscoelasticity as well as apparent wall slip effects at high shear rates have been studied. Especially, the variation of these parameters with increasing solids content is discussed in order to account for the dewatering of the color during the coating process.

2 Samples

The recipes for the coating colors investigated, standard viscosity and water retention data and solids content are given in Tabs. A 1–A 3 of Appendix A. Technical data of machine trials and the resulting runnability properties of the different colors are summarized in Tabs. A 4 and A 5 of Appendix A. A clear ranking with respect to their runnability is found:

color #1 (worst) < #2 < #3 < #4 (best)

3 Experimental Methods

High shear viscosity data were determined using a homemade piston-driven capillary viscometer (Fig. 1 a). With

* Dr. N. Willenbacher (author to whom correspondence should be addressed), Polymer Research Division, BASF AG, Dr. H. Hanciogullari, Dispersions Division, BASF AG, Dr. Hans Günther Wagner, Engineering Research and Development, BASF AG, D-67056 Ludwigshafen, Germany.

0930-7516/97/0811-0557 $17.50+.50/0

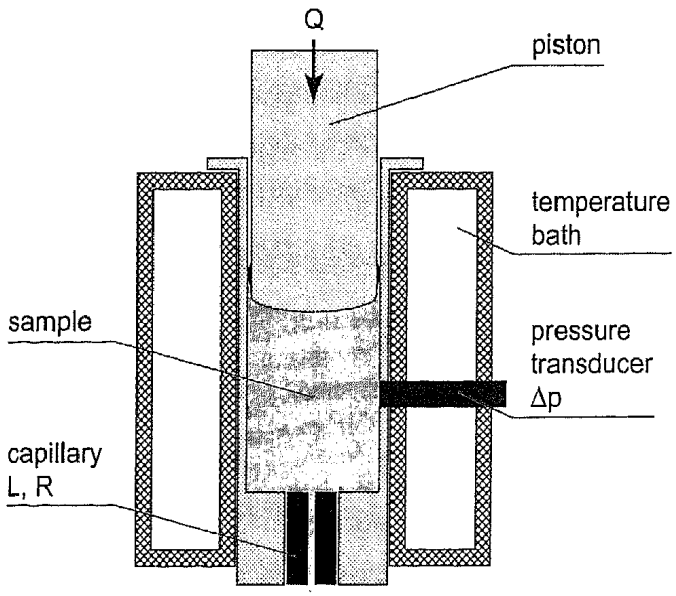

Figure 1a. Schematic drawing of our homemade piston-driven capillary viscometer.

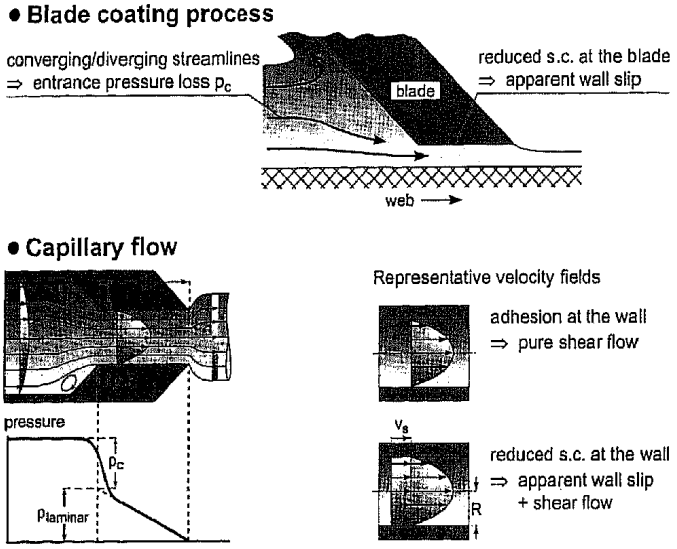

Figure 1b. Analogy between capillary flow and the flow before and under the blade.

this instrument the coating is extruded from a thermostatted reservoir through a cylindrical die of length L and radius R.

The volumetric flow rate Q through the capillary is controlled by the velocity of the piston (cross section: 12.5 mm; speed range: 0.016–16 mm/s). The resulting pressure drop p is obtained by a transducer mounted to the sample reservoir about 20 mm above the entrance of the capillary. Thus, the total pressure drop measured includes the pressure loss along the capillary as well as pressure loss effects occurring at the capillary entrance.

The analysis of paper coating capillary viscometry data has been discussed thoroughly by Laun and Hirsch [2]. The basic results are summarized briefly in Appendix B.

As shown schematically in Fig. 1b, the flow field in a capillary viscometer is very similar to the flow at and under the blade in the paper coating process and apart from the high shear viscosity, which is correlated to the pressure drop along the capillary, two more coating color properties which can affect the runnability have been determined:

1) the pressure loss p_c due to the convergence of stream lines at the entrance of the blade,
2) apparent wall slip effects due to a depletion of pigment particles in the vicinity of the blade.

4 Results and Discussion

4.1 High Shear Viscosity

4.1.1 Initial Solids Content

High shear viscosity data for the coating colors at their initial solids content are shown in Fig. 2a. The data were obtained using a standard capillary (L=150 mm, R=0.3 mm) routinely used in our laboratory for paper coating characterization. None of the corrections mentioned in Appendix B have been made here.

All colors except #4 show a slight shear thinning in the shear rate range investigated and the viscosity level decreases from color #1 to #4 in accordance with rotational viscometry data (Appendix A).

4.1.2 Simulation of the Blade Geometry

With respect to the dimensions of the blade coater gap the extrusion behavior of the colors has been investigated using a short capillary with a circular cross section and L/R=10 (about the same ratio of blade length to gap height is typical for the blade coating process). For shear rates close to $10^6\ s^{-1}$ the extrusion pressure is dominated by entrance pressure losses, which for these colors are obviously well approximated by Eq. (6). Hence, the extrusion pressure increases proportionally to $\dot{\gamma}^2$ and is independent of coating color viscosity (Fig. 2b). No laminar flow profile is formed in such a short die at very high shear rates. As a consequence, the runnability behavior should be similar for these coating colors, if it was determined by the flow properties of the colors at their initial solids content. But note, the colors partially dewater before and under the blade gap. Therefore, the viscosity under the blade is increased and, accordingly, the critical shear rate above which entrance pressure losses dominate increases, too.

4.1.3 Variation of Solids Content

The effect of solids content on high shear viscosity has been investigated for coatings #1 and #4. For each coating four different concentrations have been prepared (Tab. A3, Appendix A). High shear viscosity data of these samples are

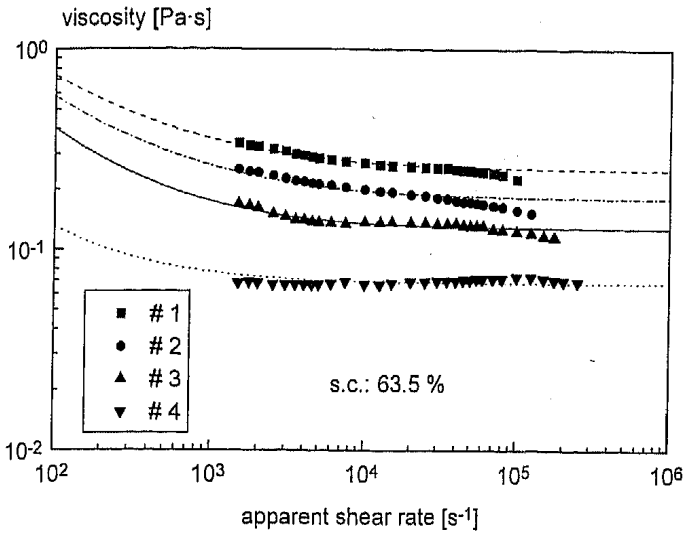

Figure 2a. High shear viscosity of fresh coating colors (capillary: R=0.3 mm; L/R=469). The lines represent fits of the Carreau model [8] to the experimental data.

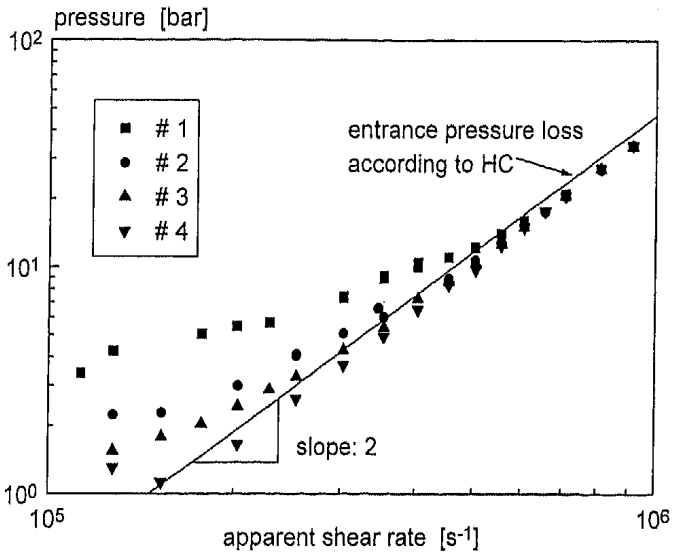

Figure 2b. Extrusion pressure vs. apparent shear rate for colors #1–#4 (capillary: R=0.2 mm, L/R=10). Solid line: HC correction according to Eq. (6).

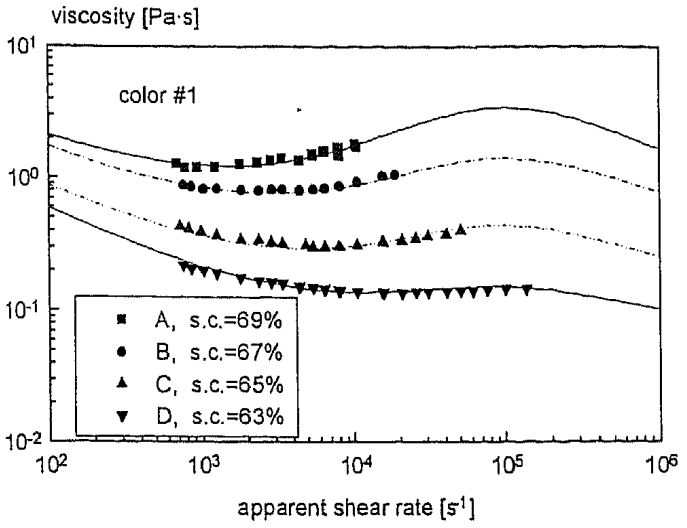

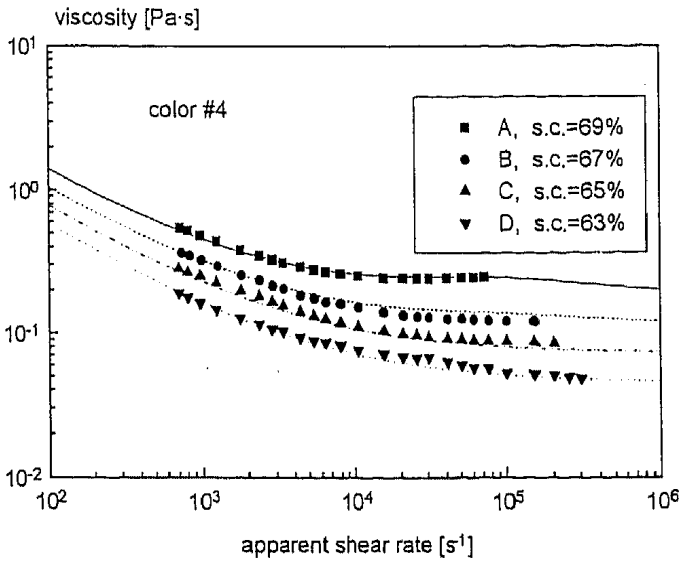

Figure 3. High shear viscosity data of coating colors #1 and #4 at various concentrations (capillary: R=0.3 mm; L/R=469).

given in Fig. 3. Obviously, the maximum shear rate attainable decreases with increasing sample viscosity due to the limitations of the pressure transducer (maximum pressure: 200 bar). Again, a standard capillary (L=150 mm, R=0.3 mm) was used and no corrections were made.

The most striking result is that for coating #1 the high shear viscosity increases with increasing solids content much stronger than for color #4. This is especially important since the water retention of color #4 is much better than that of color #1 (see Tab. A2). Therefore, the viscosity difference between these colors in the coating process is even higher than expected from a comparison of the viscosity data at a certain concentration. Moreover, coating #1 shows a pronounced shear thickening except for the lowest concentration, whereas coating #4 is (slightly) shear thickening only at the highest concentration investigated. The lines shown in Fig. 3 represent fits of a linear superposition of the Carreau model and the Gillespie model [9] to the experimental data. The latter was used to describe the dilatancy contribution to the flow curves.

4.2 *Entrance Pressure Loss Effects*

The entrance pressure losses p_c have been obtained from capillary rheometry according to Bagley's method (Appendix B). In Fig. 4 the experimentally determined p_c values are plotted vs. apparent shear rate $\dot{\gamma}_a$. In all cases, p_c increases proportionally to $\dot{\gamma}^2$ similar to the HC correction for Newtonian fluids (calculated from Eq. (6)) which is also shown.

At low solids content (colors #1D and #4D) the experimentally determined p_c values are fairly well approximated by the HC correction. Therefore, these colors can be treated as purely viscous shear thinning fluids.

At high solids content (colors #1A, #4A) the experimental p_c values are much higher than predicted by Eq. (6).

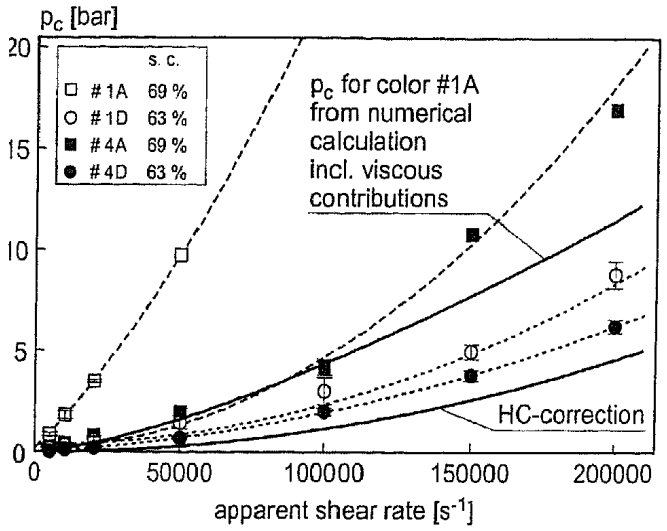

Figure 4. Experimentally determined entrance pressure losses. Dashed/dotted lines: quadratic polynomials fitted to the experimental data. Lower solid line: HC correction according to Eq. (6). Upper solid line: Numerically calculated entrance pressure loss for color #1 A including viscous contributions.

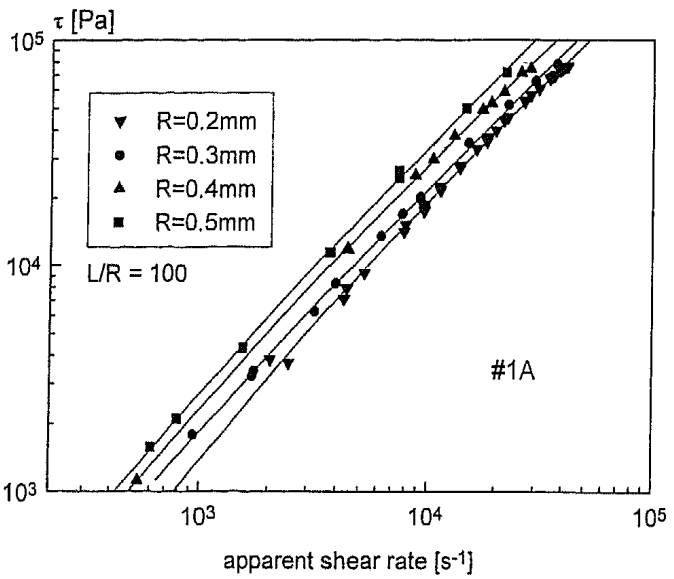

Figure 5. True wall shear stress vs. apparent shear rate for dies with different radii but const. *L/R*. Lines: Polynomial fits needed to perform the Mooney analysis.

Similar observations are reported by Wilson and Greenblatt [5], but, in contrast to their findings, p_c here always increases as $\dot{\gamma}^2$ and, therefore, these phenomena will be even more important at the high shear rates occurring under the blade coater gap than in the shear rate range accessible here.

For color #4A viscous contributions to p_c can be neglected (as well as for colors #1D and #4D) and Eq. (6) is an upper boundary for p_c as long as the color is assumed to be a purely shear thinning fluid. For color #1A, which has a much higher viscosity than the other samples considered in this section, we have calculated the viscous contribution to p_c numerically (as described in Appendix B) using the viscosity data shown in Fig. 3 as input parameters. The variation of the computed entrance pressure loss with shear rate is also shown in Fig. 4. The experimental data for color #1A exceed even this calculated pressure drop drastically. The experimentally observed excess entrance pressure losses for colors #1A and #4A cannot be predicted as long as the colors are treated as purely viscous shear thinning fluids. Therefore, it is concluded that these coating colors are viscoelastic at high solids contents and high shear rates.

Finally, it is emphasized that the increase of p_c with increasing solids content is much more pronounced for color #1 than for color #4.

4.3 Apparent Wall Slip

Apparent wall slip effects have been analyzed after correcting the experimental data for entrance pressure loss effects (Bagley correction for coatings #1A and #4A, HC-correction for coatings #1D and #4D).

Table 1. Apparent slip velocity, corrected shear rate and slip coefficient for colors #1 and #4.

Color #	s.c. [%]	v_s [m/s]$^{+)}$	$\dot{\gamma}_c$ [s^{-1}]$^{+)}$	$Ws^{*)}$
1A	69	1.0	10000	10.0
1D	63	3.5	225000	1.6
4A	69	5.0	255000	1.9
4D	63	11.5	575000	2.0

+) $\tau = 5 \cdot 10^4$ Pa; *) $R = 0.04$ mm.

Shear stress vs. shear rate curves for coating #1A obtained with dies of different radii (Fig. 5) show a significant increase of viscosity with increasing radius, indicating a pronounced apparent wall slip. The corrected shear rate $\dot{\gamma}_c$ and the slip velocity v_s were determined from Mooney plots as described in Appendix B. Both quantities increase linearly with increasing shear stress. The data for $\tau = 5 \cdot 10^4$ Pa are summarized in Tab. 1.

It is convenient to characterize the relevance of the apparent wall slip in capillary flow by the dimensionless slip coefficient *Ws*, which is defined as the ratio of the slip velocity v_s and the mean velocity $\bar{v}$ of a volume element due to the pure shear flow. In other words, it gives the ratio of the mass transport due to the slip-induced plug flow and the true shear flow:

$$Ws = \frac{v_s}{\bar{v}} = \frac{4\,v_s}{\dot{\gamma}_c}\,\frac{1}{R} \tag{1}$$

Ws increases proportionally to R^{-1}, reflecting that the apparent wall slip is getting more important with decreasing die radius. We have calculated *Ws* for the colors investigated here with the data from Tab. 1 and inserting $R = 0.04$ mm, which corresponds to a typical gap height in the blade coating process. The resulting coefficients are also given in Tab. 1. For both colors the apparent wall

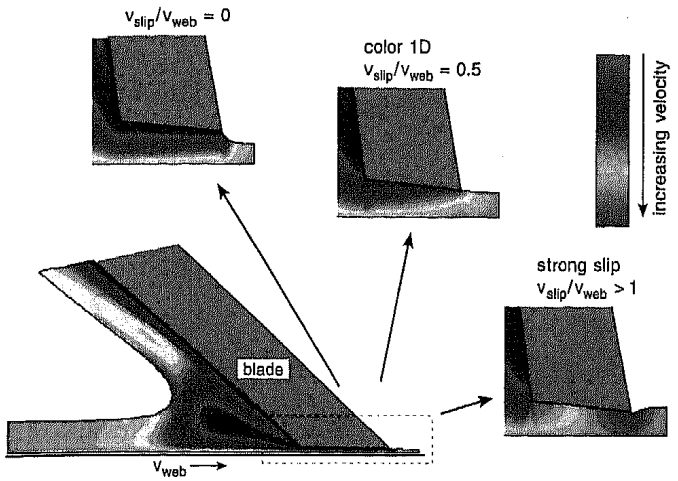

Figure 6. Effect of wall slip on the velocity field under the blade for Re=10. All other operating parameters and blade geometry as in [10].

slip is dominating the fluid transport in such a small gap, since in all cases $Ws > 1$. For color #1 the slip coefficient increases strongly with increasing solids content, while it remains essentially independent of concentration for color #4.

Note, at shear rates/stresses as high as in the coating process slip velocities may occur which are close to or even higher than the web velocity. Therefore, it is assumed that the slip phenomenon may play an important role in the blade coating process. We have calculated its effect on the flow field under the blade again using the commercial CFD code FIDAP™ [10]. Typical results are shown in Fig. 6. Introducing slip changes the shape and thickness of the free coating layer behind the blade. If $v_s > v_{web}$, the fluid speed is higher at the blade tip than at the web, and the velocity vectors at the blade tip have components directed perpendicularly to the web plane. Therefore, the surface gets instable and it is speculated that this effect may be correlated to spraying and spitting phenomena which are often observed in the coating processes. This topic will have to be examined carefully in the future.

5 Summary and Recommendation

A thorough discussion of the high shear rheology of four coating colors with significantly different runnability is presented here. In addition to the high shear viscosity, entrance pressure losses and apparent wall slip effects have been studied at various solids contents in order to account for the dewatering of the color during the coating process.

Coating color #1 with a poor runnability exhibits a high viscosity at high shear rates. The viscosity itself but also the entrance pressure loss p_c and the apparent wall slip coefficient *Ws* are strongly increasing with increasing solids content.

Color #4 with the best runnability properties shows a lower viscosity and its increase with increasing solids content is much smaller than for coating #1. The increase of p_c is also less pronounced than for color #1 and the slip coefficient *Ws* is practically independent of solids content. The high entrance pressure losses observed at increased solids content are interpreted as a viscoelastic effect occurring at high shear rates.

In the coating process, the observed rheological differences will even be enhanced, since the water retention of color #4 is much better than that of color #1 (see Tab. A2), which in turn is expected to exhibit a much stronger increase of solids content during the application process.

For the samples investigated here, all rheological properties are changing simultaneously with changing coating color recipe and it is not possible to separate out the contribution of the particular rheological features on the runnability of the coating colors or to correlate the runnability to a single rheological parameter. This demonstrates the complexity of this problem, and indeed, one will need a large amount of data from carefully selected coating formulations in order to establish the desired correlations.

On the other hand, one can try to get these correlations from a numerical analysis of the coating process [4]. We have started to figure out the effect of water retention via its effect on rheology on the runnability of a coating color by such numerical simulations [8]. Future experimental work will concentrate on an appropriate characterization of the dewatering kinetics of coating colors under process-relevant conditions in order to provide a profound basis for these calculations.

Appendix A

Composition and Runnability Characteristics of the Investigated Colors

Table A1. Coating color recipes.

	#1	#2	#3	#4
Fine English clay	100	60	60	60
Fine ground $CaCO_3$	–	40	40	40
NaOH	0.05	0.05	0.05	0.05
XSB binder Styronal PR 8669	10	10	10	–
Styronal D 708	–	–	–	10
Cobinder A	0.18	0.3	–	–
Cobinder B	–	–	0.5	0.5

Table A2. Standard viscosity data, pH, solids content and water retention.

	#1	#2	#3	#4
pH	8.8	8.5	8.7	8.7
s.c. (%)	63.5	63.7	63.8	63.3
Brookfield (mPas)				
spindle 4, 20 rpm	4420	3000	5300	4800
100 rpm	1590	1130	1630	1380
High-shear viscosity (mPas) (Haake, $\dot{\gamma}=17500\ s^{-1}$)	269	113	117	93
Water retention (g/m^2)*)	113	125	72	68

*) Kaltec/Gradek method, pressure: 0.5 bar; time: 60 s.

Table A3. Variation of solids content and density of coating colors #1 and #4.

Sample	1A	1B	1C	1D	4A	4B	4C	4D
s.c./%	69.0	67.3	65.3	63.3	68.8	66.8	65.2	62.9
ρ/g cm^{-3}	1.53	1.53	1.49	1.48	1.63	1.62	1.59	1.56

Samples #1D and #4D correspond to samples #1 and #4 in Tab. 1.

Table A4. Technical data of machine trials.

Pilot Coating Machine II GSM 2000 Jagenberg at BASF Technical Center
Working width: 800 mm; application system GSM 2000: Roll applicator
Stiff blade (blade angle 42°; bevel angle 40°; free length 16 mm; thickness 0.38 mm)
Base paper: wood-free 70 g/m^2

	#1	#2	#3	#4
Blade loading (mm)				
at 600 m/min	2.69	2.78	2.67	2.19
at 1600 m/min	7.62*)	7.40	6.81	6.24
Coat weight (g/m^2)	12.4	12.1	12.9	12.4
Moisture content (%)	4.53	4.04	4.06	4.06

*) at 1400 m/min.

Table A5. Runnability characteristics.

Machine speed	#1	#2	#3	#4
1200 (m/min)	strong bleeding, spraying (getting worse)	strong bleeding, slightly spraying	strong bleeding	slight bleeding
1400 (m/min)	stop of trial	strong bleeding, spraying	strong bleeding, slightly spraying	slight bleeding
1600 (m/min)	–	stop of trial	strong bleeding, spraying	strong bleeding, spraying

Appendix B

Evaluation of Rheological Quantities from Capillary Viscometry Raw Data

B1 Viscosity

Assuming Newtonian flow behavior the apparent wall shear rate $\dot{\gamma}_a$ is calculated from Q according to

$$\dot{\gamma}_a = \frac{4Q}{\pi R^3} \tag{2}$$

The true wall shear stress τ is related to the pressure drop p by

$$\tau = \frac{p - p_c}{2L/R} \tag{3a}$$

where p_c accounts for additional pressure losses at the entrance and exit of the die which have to be subtracted from the total pressure given by the transducer (mounted above the entrance of the capillary) in order to obtain the pressure loss due to the laminar flow in the die. In many practical applications it is sufficient to choose L/R large enough, so that $p \gg p_c$ and

$$\tau = \frac{p}{2L/R} \tag{3b}$$

The apparent viscosity η_a is defined as

$$\eta_a = \frac{\tau}{\dot{\gamma}_a} \tag{4}$$

and, finally, the true viscosity $\eta\ (\dot{\gamma})$ is obtained by a simple rescaling of the shear rate:

$$\eta(\dot{\gamma}) = \eta_a(\dot{\gamma}_a) \quad \text{for} \quad \dot{\gamma} = 0.83\,\dot{\gamma}_a \tag{5}$$

This approximation does not differ significantly from the mathematically exact Rabinowitsch-Weissenberg correction.

B2 Entrance Pressure Loss

First we assume that viscous contributions to the entrance pressure loss are negligible. Then for *Newtonian fluids* the entrance pressure loss p_c is mainly due to three effects:

- acceleration of the fluid from about zero velocity in the reservoir to the mean velocity in the die
- contraction of stream lines at the entrance of the capillary
- deformation of the flow field from a plug flow (within the reservoir) to a parabolic flow profile (within the die)

and is approximately given by [11]

$$p_c = \frac{1.27\,\rho R^2 \dot{\gamma}_a^2}{16} \tag{6}$$

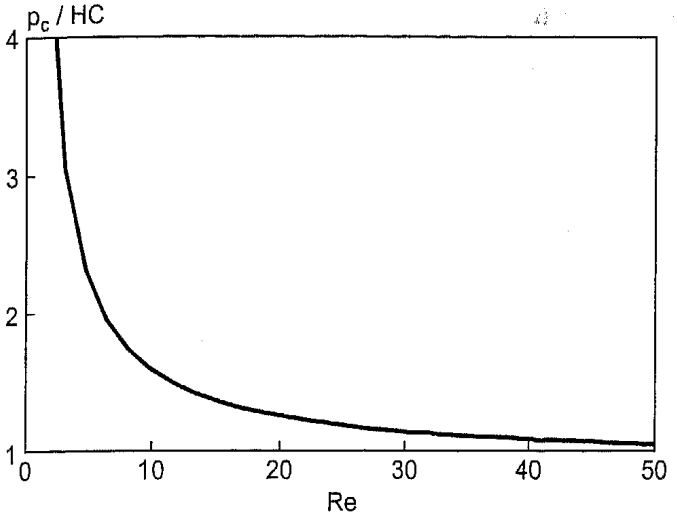

Figure 7. Numerically calculated total entrance pressure loss p_c for a Newtonian fluid in capillary flow normalized by the Hagenbach-Couette term (HC) from Eq. (6) (piston radius: 12.5 mm; die radius: 0.3 mm, cf. Fig. 1 a).

which is called Hagenbach-Couette (HC) correction or kinetic energy correction.

For *purely viscous, but shear thinning fluids* p_c is overpredicted by Eq. (6) since the deformation of the flow profile in the capillary is less pronounced.

In the case of *viscoelastic fluids* an increased resistance to the converging elongational flow at the die entrance can occur which is difficult to predict theoretically since it requires a constitutive equation which has not yet been established for concentrated colloidal systems like paper coating colors. But viscoelasticity can show up experimentally as an increased resistance to the converging (elongational) flow at the entrance of the capillary, leading to an excess entrance pressure loss, which is significantly larger than predicted by Eq. (6). As a consequence, measuring p_c is a valuable tool to characterize viscoelastic coating properties at high shear rates, which are otherwise hardly accessible.

The entrance pressure loss p_c is determined experimentally from measurements with capillaries of different L/R but similar radius. For constant $\dot{\gamma}_a$ the resulting extrusion pressure p is plotted versus L/R (Bagley plot) and p_c is obtained from a linear extrapolation of corresponding data points to $L=0$ (intercept with the p-axis).

In contrast to the above assumption, the viscous contribution to the entrance pressure loss may not be neglected if the Reynolds number $\mathrm{Re}=\frac{2\rho Q}{\pi R\eta}$ of the flow is low. For a Newtonian fluid this effect has been checked numerically using the commercial CFD code FIDAP™. A typical die geometry (die radius: 0.3 mm, sample reservoir radius: 12.5 mm) and adhesion of the fluid at the wall have been assumed. The input parameters fluid viscosity and piston velocity have been varied. The resulting entrance pressure loss (Fig. 7) exceeds the Hagenbach-Couette prediction (Eq. (6)) drastically for Reynolds numbers $\mathrm{Re}<10$. That is, at such low Reynolds numbers viscous contributions to p_c have to be considered. This is discussed in more detail in Section 4.2.

B 3 Apparent Wall Slip

For heterogeneous systems like coating colors another effect has to be considered. Geometrical packing restrictions near the wall, a shear-induced particle migration or a specific interaction between the wall and the constituents of the coating color can lead to a reduced solids content in the vicinity of the capillary wall. This again can cause the formation of a slip plane or a narrow region of high shear rates resulting in a systematic decrease of the apparent viscosity with decreasing die radius. The corresponding flow field can be interpreted in terms of a linear superposition of a plug flow, characterized by an apparent wall slip velocity v_s, and a laminar shear flow, characterized by a corrected shear rate $\dot{\gamma}_c$. If the apparent slip velocity solely depends on the wall shear stress, the apparent shear rate can be expressed as

$$\dot{\gamma}_a = \dot{\gamma}_c + \frac{4}{R} v_s \tag{7}$$

Accordingly, the slip effect is separated from the viscous flow by comparing flow curves determined with dies of different radii but similar L/R. Plotting the apparent wall shear rate versus $4/R$ for constant wall shear stress (Mooney plot) then yields a straight line and $\dot{\gamma}_c$ and v_s are given by the intercept (with the $\dot{\gamma}_a$-axis) and the slope of this line, respectively.

Acknowledgement

We thank R. Benz and D. Lingenfelder for carefully performing the experiments. Many fruitful discussions with Dr. H.M. Laun are greatly acknowledged. F. Brotz is thanked for performing the numerical calculations.

Received: July 22, 1997 [CET 937]

References

[1] Kuzmak, J.M., *Tappi Journal 69* (1986) No. 2, p. 72.
[2] Laun, H.M., Hirsch, G., *Rheologica Acta 28* (1989) p. 267.
[3] Sandas, S.E., Salminen, P.J., *Tappi Journal 74* (1991) No. 12, p. 79.
[4] Roper, J.A., Attal, J.F., *Tappi Journal 76* (1993) No. 5, p. 55.
[5] Wilson, T.S., Greenblatt, G.D., *Proceedings of the ACS Division of Polymeric Materials Science and Engineering 73* (1995) p. 484.
[6] Bergh, N.O., Hemmes, J.L., *Wochenblatt für Papierfabrikation* 2 (1996) p. 57.
[7] Weigl, J., Laber, A., Wittig, O., *Wochenblatt für Papierfabrikation 5* (1996) p. 161.
[8] Barnes, H.A., Hutton, J.F., Walters, K., *An Introduction to Rheology*, Elsevier, Amsterdam 1989.
[9] Gillespie, J.T., *Journal of Colloid Science 22* (1966) p. 554.
[10] Brotz, F., Wagner, H.G., Hanciogullari, H., *Proceedings of the TAPPI Coating Fundamentals Symposium*, Philadelphia 1997.
[11] Böhme, G., *Strömungsmechanik nicht-newtonscher Fluide*, Teubner, Stuttgart 1981.